The Plant Cell, Vol. 19: 2719–2735, September 2007, www.plantcell.org

The *Arabidopsis* BEL1-LIKE HOMEODOMAIN Proteins SAW1 and SAW2 Act Redundantly to Regulate *KNOX* Expression Spatially in Leaf Margins [W]

Ravi Kumar,[1] Kumuda Kushalappa,[1] Dietmute Godt, Mark S. Pidkowich, Sandro Pastorelli, Shelley R. Hepworth,[2] and George W. Haughn[3]

Department of Botany, University of British Columbia, Vancouver, British Columbia, V6T 1Z4 Canada

In *Arabidopsis thaliana*, the BEL1-like TALE homeodomain protein family consists of 13 members that form heterodimeric complexes with the Class 1 KNOX TALE homeodomain proteins, including SHOOTMERISTEMLESS (STM) and BREVIPEDICELLUS (BP). The BEL1-like protein BELLRINGER (BLR) functions together with STM and BP in the shoot apex to regulate meristem identity and function and to promote correct shoot architecture. We have characterized two additional BEL1-LIKE HOMEODOMAIN (BLH) proteins, SAWTOOTH1 (BLH2/SAW1) and SAWTOOTH2 (BLH4/SAW2) that, in contrast with BLR, are expressed in lateral organs and negatively regulate *BP* expression. *saw1* and *saw2* single mutants have no obvious phenotype, but the *saw1 saw2* double mutant has increased leaf serrations and revolute margins, indicating that SAW1 and SAW2 act redundantly to limit leaf margin growth. Consistent with this hypothesis, overexpression of *SAW1* suppresses overall growth of the plant shoot. *BP* is ectopically expressed in the leaf serrations of *saw1 saw2* double mutants. Ectopic expression of Class 1 *KNOX* genes in leaves has been observed previously in loss-of-function mutants of *ASYMMETRIC LEAVES* (*AS1*). Overexpression of *SAW1* in an *as1* mutant suppresses the *as1* leaf phenotype and reduces ectopic *BP* leaf expression. Taken together, our data suggest that BLH2/SAW1 and BLH4/SAW2 establish leaf shape by repressing growth in specific subdomains of the leaf at least in part by repressing expression of one or more of the *KNOX* genes.

INTRODUCTION

Morphogenesis in plants is achieved primarily through the regulation of differential growth in distinct domains of a developing organism. Such differential growth is specified by transcription factors expressed in specific domains in response to positional information. Among the transcription factors that regulate morphogenesis are members of the BEL1-LIKE HOMEODOMAIN (BLH) and KNOTTED1-LIKE HOMEOBOX (KNOX) TALE (for three amino acid loop extension) homeodomain protein families.

In *Arabidopsis thaliana*, two key members of the KNOX family whose functions have been defined are SHOOTMERISTEMLESS (STM), required for meristem maintenance and/or function (Barton and Poethig, 1993; Long et al., 1996), and BREVIPEDICELLUS (BP/KNAT1), required for regulation of inflorescence architecture (Douglas et al., 2002; Venglat et al., 2002). The *Arabidopsis* BLH proteins BELLRINGER (also called PENNYWISE, REPLUMLESS, VAAMANA [BLR/PNY/RPL/VAM]) and its paralog POUNDFOOLISH (PNF) play similar roles in shoot development and exhibit functional redundancy in these roles (Byrne et al., 2003; Smith and Hake, 2003; Bao et al., 2004; Bhatt et al., 2004; Smith et al., 2004).

KNOX proteins interact with specific members of BLH proteins in *Arabidopsis* (Bellaoui et al., 2001; Byrne et al., 2003; Smith and Hake, 2003; Bhatt et al., 2004; Hackbusch et al., 2005; Kanrar et al., 2006). Such interactions have been shown to be required for site-specific DNA binding (Smith et al., 2002) and for nuclear localization of the transcription factor heterodimeric complex (Bhatt et al., 2004; Cole et al., 2006). Analogous BLH–KNOX interactions have also been reported in other plants, such as potato (*Solanum tuberosum*) and barley (*Hordeum vulgare*), indicating that these interactions are evolutionarily conserved and that the interaction is probably required for their biological functions (Muller et al., 2001; Chen et al., 2003).

The *Arabidopsis* BEL1 protein, required for ovule morphogenesis (Robinson-Beers et al., 1992; Modrusan et al., 1994), also interacts with BP and other KNOX proteins in yeast and in vitro (Bellaoui et al., 2001; Hackbusch et al., 2005). *bel1* loss-of-function mutants have abnormal ovules due to defects in integument differentiation (Robinson-Beers et al., 1992; Modrusan et al., 1994). However, no KNOX-derived functions have been attributed to the mediation of BEL1-mediated ovule morphogenesis. Although the *BEL1* gene is expressed in stems, leaves, sepals, inflorescence meristems, roots, and ovules (Reiser et al., 1995; Bellaoui et al., 2001; this study), no obvious phenotypes outside the ovule are visible in *bel1* knockout lines. The lack of phenotypes in these other tissues might be attributable to the presence of other BLH proteins whose functions overlap with

[1] These authors contributed equally to this work.
[2] Current address: Department of Biology, Carleton University, 1125 Colonel By Drive Ottawa, Ontario, Canada, K1S 5B6.
[3] Address correspondence to haughn@interchange.ubc.ca.
The author responsible for distribution of materials integral to the findings presented in this article in accordance with the policy described in the Instructions for Authors (www.plantcell.org) is: George W. Haughn (haughn@interchange.ubc.ca).
[W] Online version contains Web-only data.
www.plantcell.org/cgi/doi/10.1105/tpc.106.048769

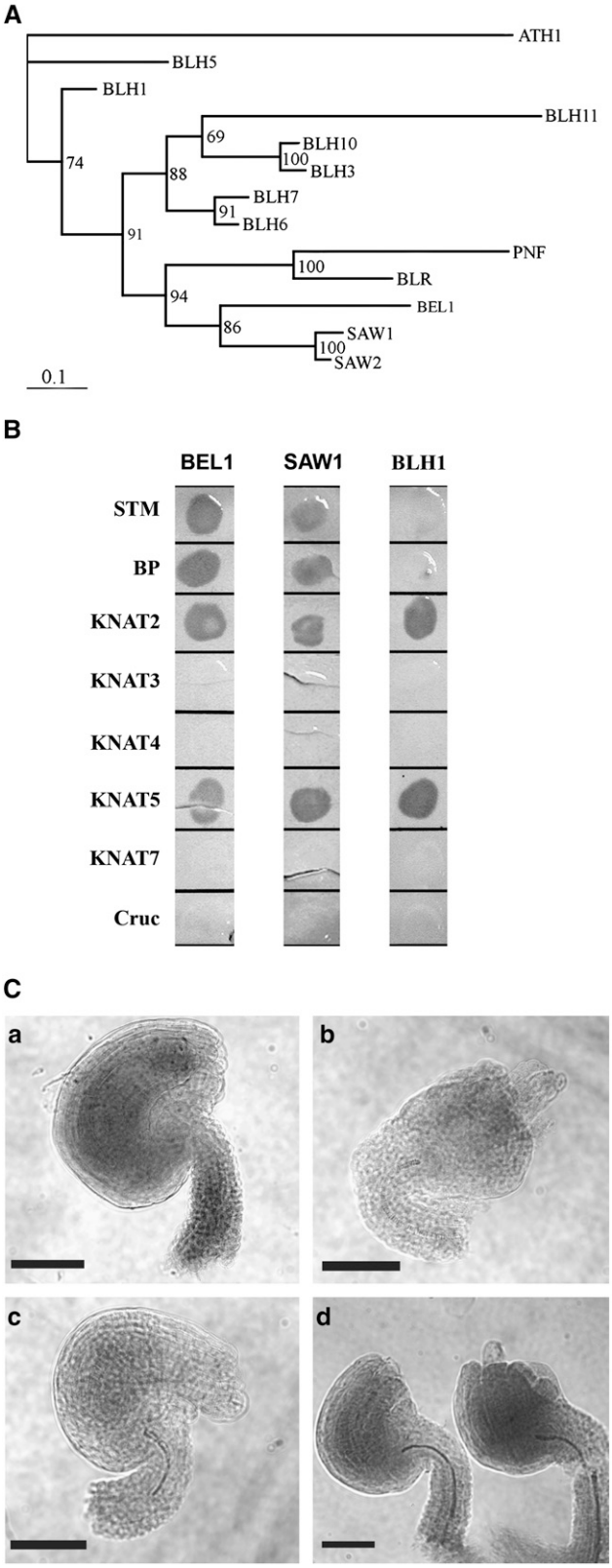

Figure 1. SAW and BEL1 Proteins Exhibit Sequence Similarity and Functional Redundancy.

(A) Phylogram of the 13 members of the BLH protein family. Bootstrap values are shown at the branch points.

(B) Yeast two-hybrid X-Gal filter assay showing interactions of BLH and KNOX proteins. The BLH proteins were used as baits and KNOX proteins as preys. Cruc, Cruciferin (negative control).

(C) Whole mounts of mature ovules showing complementation of the *bel1* mutant by *35S:SAW1*. (a) The wild type (b) *bel1-3*, (c) *35S:SAW1*, and (d) *35S:SAW1 bel1-3*. Bars = 50 μm.

that of BEL1. To investigate this possibility, we have used a reverse genetics approach to begin to unravel the redundancy that we show exists in the BLH family.

In this study, we describe the characterization of two BLH proteins, SAWTOOTH1 (SAW1) and SAW2 (formerly called BLH2 and BLH4, respectively) that show significant amino acid sequence similarities with BEL1. The two SAW proteins are functionally redundant. The *saw* double mutants exhibit increased leaf serrations, giving the leaf margin a saw-like appearance. The leaf margins are also more revolute (abaxially curled) than the wild type. Overexpression of *SAW1* impedes general growth of the plant. Molecular and genetic analyses reveal that the SAW proteins function in part by repressing *BP* (and other Class I *KNOX* genes) expression in the leaves.

RESULTS

BEL1, SAW1, and SAW2 Are Members of the BELL Family of Homeodomain Proteins

The loss of *BEL1* gene function results in abnormal ovule growth and embryo sac arrest (Robinson-Beers et al., 1992; Modrusan et al., 1994). Consistent with its mutant phenotype, *BEL1* is expressed in the developing ovule and in the inflorescence apex (Reiser et al., 1995; Bellaoui et al., 2001). However, RNA gel blot (Reiser et al., 1995) and in situ hybridization (Bellaoui et al., 2001) indicate that *BEL1* is expressed in vegetative tissues where there is no obvious mutant phenotype. This lack of vegetative phenotype in a *bel1* null mutant could be explained by genetic redundancy. In *Arabidopsis*, there are 12 TALE homeobox genes closely related in sequence to *BEL1* that have been identified, including *BLH1-7*, *BLH10*, *BLH11* (for *BEL1-LIKE HOMEODOMAIN*), *BLR*, *PNF*, and *ATH1* (Quaedvlieg et al., 1995; Reiser et al., 1995; Bellaoui et al., 2001; Becker et al., 2002; Byrne et al., 2003; Roeder et al., 2003; Smith and Hake, 2003; Smith et al., 2004; Hackbusch et al., 2005; this study). These deduced BLH proteins share at least three regions of sequence similarity: the DNA binding homeodomain and the BELL and SKY domains involved in BEL1 interactions with KNOX TALE homeodomain proteins (Bellaoui et al., 2001; Becker et al., 2002). Phylogenetic analysis of this gene family (Figure 1A; Becker et al., 2002) indicates that the genes most closely related in sequence to *BEL1* are two genes formerly referred to as *BLH2* and *BLH4* (Becker et al., 2002) that we designate *SAW1* and *SAW2*, respectively, based on their loss-of-function leaf phenotype (see below). We focused on these two genes as the ones most likely to have overlapping functions with BEL1, similar to the situation observed with *Arabidopsis* MADS domain proteins (Pelaz et al., 2000). SAW1

and SAW2 proteins are 87% identical. The *BEL1* gene is more closely related to *BLH2*/*SAW1* and *BLH4*/*SAW2* than to other BLH genes (Figure 1A; 73 and 72% protein sequence similarity, respectively). *SAW2* and *SAW1* are on chromosomes 2 and 4, respectively, and the chromosomal regions surrounding these genes share extensive sequence similarity (Table 1; see Supplemental Figure 1B online; Blanc et al., 2003), suggesting that they arose from segmental chromosomal duplication of one of the two loci. Since *SAW1* and *SAW2* exhibit sequence similarity, it is possible that the two genes share similar functions and exhibit similar expression patterns. Indeed, a comparison of the regions upstream to the translational start sites of *SAW1* and *SAW2* genes shows three conserved regions in the 5′ untranslated region (see Supplemental Figure 1C online), indicating that they might have common transcriptional and posttranscriptional regulatory elements. In support of this hypothesis, results of a PRIMe microarray coexpression gene search (http://prime.psc.riken.jp/?action=coexpression_index) with one of the two genes identifies the other as the best coexpression match, indicating that the two genes are expressed in similar domains.

SAW1, but Not BLH1, Interacts with the Same KNOX Proteins as BEL1

We have previously reported that BEL1 selectively interacts with KNOX homeodomain proteins and that this interaction primarily involves the SKY and BELL domains (Bellaoui et al., 2001). Since these domains are highly conserved between BEL1, SAW1, and SAW2 proteins, it is possible that their ability to interact with KNOX proteins is also similar. To test this hypothesis, full-length cDNAs for *BEL1*, *SAW1*, and a more distantly related gene *BLH1* were used in yeast two-hybrid assays as prey (TA) to test for interaction with KNAT homeodomain proteins and the seed storage protein Cruciferin (negative control) as bait (DB). As anticipated from previous results (Bellaoui et al., 2001), BEL1 was able to interact with STM, BP, KNAT2, and KNAT5 but not KNAT3, KNAT4, KNAT7, or Cruciferin. None of the BLH proteins in combination with DB-Cruciferin activated β-galactosidase, indicating that BLH proteins do not interact with GAL4 DB or nonspecifically with other proteins (Figure 1B). TA-SAW1 and TA-SAW2 promoted β-galactosidase activity in combination with DB-BP, KNAT2, KNAT5, and STM but not with DB-KNAT3, 4 or 7; an interaction profile identical to that of BEL1. However, TA-BLH1 promoted β-galactosidase activity only in combination with TA-KNAT2 and pTA-KNAT5. These data suggest that members of BLH family are generally capable of forming heterodimeric complexes with KNOX proteins but that the specific KNOX partners may vary.

SAW1, *SAW2*, and *BEL1* Are Expressed in Partially Overlapping Expression Domains

We investigated the expression domains of *SAW1* and *SAW2* in more detail using RT-PCR, RNA in situ hybridization (*SAW1* and *BEL1*), and β-glucuronidase (*GUS*) reporter constructs fused to the *SAW1*, *SAW2*, and *BEL1* promoter regions to provide clues to their function and determine the extent to which their expression domains overlap with each other and that of *BEL1* (Figure 2; see Supplemental Figure 2 online). Unlike *BEL1* (Reiser et al., 1995; Bellaoui et al., 2001), *SAW1* and *SAW2* were not expressed in developing ovules (Figures 2B and 2C) and therefore are unlikely to be redundant with BEL1 function in ovule development. These data are consistent with the fact that mutation of *BEL1* results in an ovule mutant phenotype (Reiser et al., 1995). *BEL1* is expressed in the inflorescence and floral meristems (Figure 2D; Bellaoui et al., 2001), but *SAW1* and *SAW2* are not (Figures 2E and 2F). However, in other parts of the plant, especially lateral organs, the expression domains of *BEL1*, *SAW1*, and *SAW2* overlap extensively, indicating that these proteins might play a specialized role in the development of such lateral organs. In flowers, all three genes were expressed in the sepals. *SAW1* and *SAW2*, but not *BEL1*, were expressed in the anther filament, style, and transmitting tract (Figures 2H and 2I), while only *BEL1* was expressed in the ovary walls and at the base of the flower (receptacle; Figure 2G). *SAW1* showed a unique, but faint, expression in the petals.

In developing leaves, *BEL1:GUS* was localized to the adaxial side (Figure 2J), similar to the adaxial expression observed for *SAW1* in sepals and leaves by in situ hybridization experiments (Figures 2E and 2K) and for *SAW2:GUS* in the cotyledons of a developing embryo (Figure 2L), suggesting a role for these genes in the development of lateral organ asymmetry. *SAW1*, *SAW2*, and *BEL1* were all expressed in mature leaves, with a more uniform adaxial/abaxial distribution. *BEL1* expression is fairly uniform throughout the mature leaf; however, *SAW1* and *SAW2* show higher expression in vasculature and hydathodes in comparison to the mesophyll and epidermal cells (Figures 2M to 2O), and *BEL1*, *SAW1*, and *SAW2* expression patterns also overlapped in the stem (cortex), pedicel, root, and embryo (data not shown).

Table 1. Paralogous Genes Found in the Duplicated Region That Includes *SAW1* and *SAW2*

Gene (AGI Number)	Paralog	Description	Exp	Identity	Similarity
At2g23630	At4g37160	Pectinesterase-like protein	3.8E-192	78%	87%
At2g23680	At4g37220	Cold acclimation protein homolog	1.0E-33	44%	63%
At2g23690	At4g37240	Unknown/putative protein	1.0E-28	59%	66%
At2g23760	At4g36870	BEL1-like homeobox proteins (SAW2 and SAW1)	2.9E-114	61%	70%
At2g23790	At4g36820	Hypothetical/putative protein	8.4E-100	66%	80%
At2g23800	At4g36810	Geranylgeranyl pyrophosphate synthase	1.2E-101	72%	86%

The genes were identified using the Web-based software available at http://wolfe.gen.tcd.ie/athal/index.html (Blanc et al., 2003). Various single copy genes occurring in the region due to deletions and chromosomal rearrangements have not been included. AGI, Arabidopsis Genome Initiative.

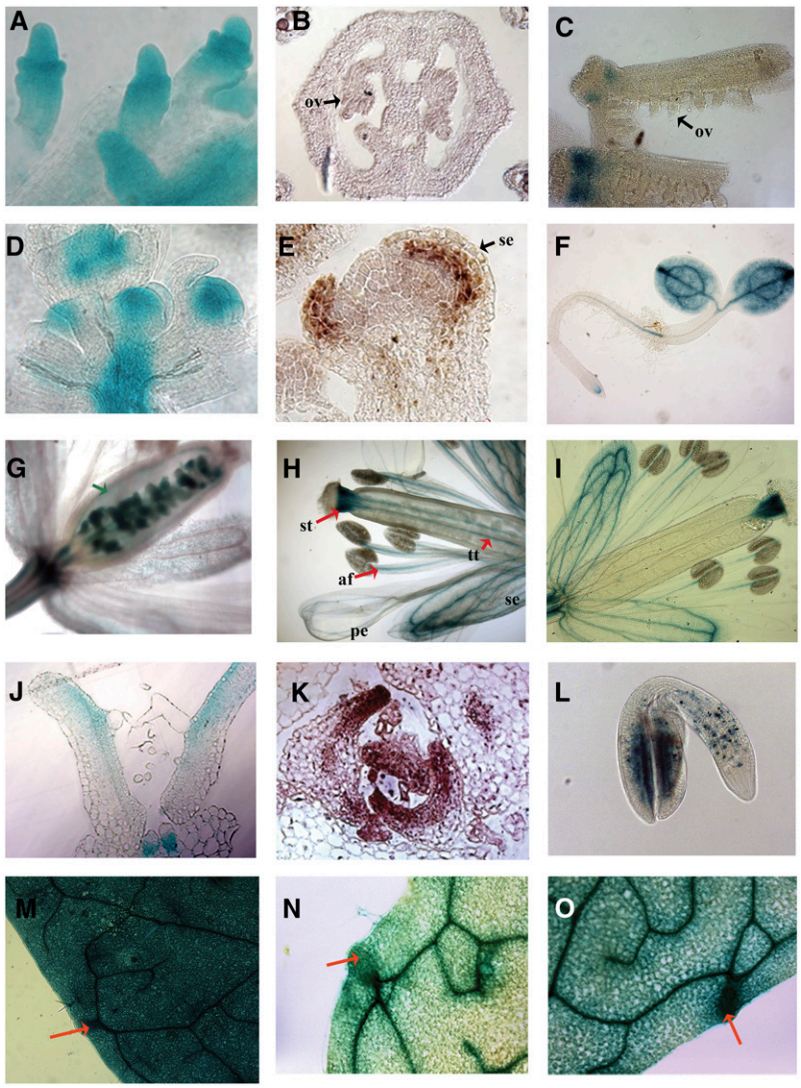

Figure 2. Expression Analysis of *SAW* and *BEL1* Genes.

(A) Immature ovules showing *BEL1:GUS* activity.
(B) *SAW1* in situ hybridization of a cross section through the gynoecium showing immature ovules (ov).
(C) *SAW2:GUS* expression in whole-mount gynoecia. One of the gynoecia was split open to reveal the immature ovules.
(D) Whole mount of the inflorescence apex. *BEL1:GUS* expression is detected in the floral meristems of immature flowers.
(E) Longitudinal section of a stage 4 flower showing *SAW1* expression (assayed by in situ hybridization) in the adaxial side of the developing sepal (se).
(F) *SAW2:GUS* expression in a 2-d-old seedling.
(G) to **(I)** Whole mounts of flowers showing *BEL1:GUS*, *SAW1:GUS*, and *SAW2:GUS* activity, respectively. st, style; tt, transmitting tract; af, anther filament; se, sepal; pe, petal.
(J) to **(L)** *BEL1*, *SAW1*, and *SAW2* exhibit adaxial expression in developing lateral organs.
(J) A longitudinal section through the vegetative apex of a 7-d-old seedling showing adaxial expression of *BEL1:GUS* in the leaves.
(K) Cross section through the vegetative apex showing in situ localization of *SAW1* in the adaxial side of developing leaves.
(L) *SAW2:GUS* expression in a developing embryo.
(M) to **(O)** Whole mounts of fifth leaves of 3-week-old plants showing *BEL1:GUS*, *SAW1:GUS*, and *SAW2:GUS* activity, respectively.

35S:SAW1 Complements the *bel1* Ovule Phenotype

Several lines of evidence suggest that SAW1 could be redundant with BEL1. To test this hypothesis directly, we introduced *35S:SAW1* into a *bel1* mutant background and evaluated its ability to complement the bel1 mutant phenotype. A *35S:SAW1* gene construct was transformed into wild-type plants. A hemizygous *35S:SAW1* transformant was crossed to *bel1-3* using *bel1-3* as a pollen donor (the *35S:SAW1* plants are male sterile; see below) and the F1 progeny backcrossed to *bel1-3*. The *bel1-3* homozygous testcross progeny were identified by PCR

(see Methods) and the ovule phenotype examined. All 18 *35S:SAW1 bel1-3/bel1-3* lines tested had ovules that appeared morphologically wild-type with both inner and outer integuments. Approximately 50% of the ovules in each silique were indistinguishable from the wild type in appearance, while the remainder had integuments that were shorter in length than the wild type (Figure 1C). Furthermore, all *35S:SAW1 bel1-3/bel1-3* lines that were cross-pollinated set seeds (data not shown), indicating that the ovules were fertile. Similar results were also obtained when *35S:SAW1* was crossed into the *bel1-1* mutant (data not shown). These results demonstrate that *35S:SAW1* can complement the *bel1-3* ovule defect.

saw1 and *saw2* Affect Leaf Margin Development

In an attempt to learn more about the function of *SAW1* and *SAW2* in planta, reverse genetic techniques were used to generate plant lines with loss-of-function *SAW1* and *SAW2* alleles. We examined *saw1* and *saw2* mutant alleles obtained through the Salk collection of T-DNA insertion lines (Alonso et al., 2003) and by screening ethyl methanesulfonate–mutagenized plants by TILLING (McCallum et al., 2000; Colbert et al., 2001; Till et al., 2004). Figure 3A shows the position of insertion/mutation in the gene in these alleles. A *SAW1* TILLING allele (*saw1-2*) had a missense mutation that would be expected to result in a nonconservative amino acid substitution that could alter the function of the encoded protein. The *saw1-1* allele has a T-DNA insertion in the third intron that separates the two exons that code for the homeodomain region. The *saw1-1* transcript is severely reduced in abundance relative to *SAW1* (Figure 3B), but transcript is still detectable. Thus, the *saw1-1* mutant could be hypomorphic. The T-DNA insertional lines, *saw2-1* and *saw2-2*, have insertions in the first intron and first exon, respectively, and have no detectable full-length transcripts (Figure 3B). All mutant alleles segregated in F2 populations as expected for single nuclear loci (data not shown). Under our normal growth conditions, no obvious morphological defects in the shoot segregated with any of the alleles examined.

Since *SAW1* and *SAW2* are products of chromosomal duplication (Table 1) and have very similar expression profiles, we suspected that the lack of visible defects in the single mutants might be because of functional redundancy and decided to examine *saw1-1 saw2-1* double mutants. Plants from an F2 population segregating for both *saw1-1* and *saw2-1* were genotyped using molecular assays (see Methods). All *saw1-1 saw2-1* double mutants, unlike the single mutants, had a distinct mutant phenotype characterized by increased serrations in leaf margins and revolute leaves that have margins curled abaxially (Figures 3C to 3E). Since in wild-type leaves *SAW1* and *SAW2* are specifically expressed in the adaxial side of developing leaves (Figures 2K and 2L) and in the hydathodes in the margins of older leaves (Figures 2N and 2O), these phenotypes could arise from loss of *SAW* function in these tissues. The *saw2* single mutants also have slightly revolute margins, but the phenotype is not as obvious as in the double mutant. On closer examination, the single mutants also show a slight increase in serration length and numbers. The serrations observed were most prominent in the seventh and subsequent leaves initiated, and these leaves have a sawtooth appearance; hence, the genes were designated as *SAW1* and *SAW2*. The double mutants had significantly more and deeper serrations than the wild type or the single mutants (Table 2). Also, the number of serrations increased with leaf number (Figure 3F). Plants heterozygous for either of the two mutations and homozygous for the other also exhibit serrations (less prominent than the double mutants), indicating that this phenotype is dosage dependant (data not shown). In addition to the leaf margin defects, *saw1-1 saw2-1* double mutant leaves are darker green in color, and the third and fourth leaves of the double mutant are more elongated than the wild-type leaves of the same stage. The plants produce more leaves than the wild type and show a delay in flowering by 2 to 3 d in our continuous light growth conditions (Table 2).

We demonstrated that the observed phenotypes were due to disruption of *saw1* and *saw2* in three ways. First, all phenotypes cosegregated with the *saw1-1 saw2-1* double mutant genotype. Second, *saw* double mutants carrying different *saw1* and *saw2* allele combinations (*saw1-1 saw2-1*; *saw1-2 saw1-1* and *saw1-1 saw2-2*) had similar phenotypes (Table 3). Third, the *saw1-1 saw2-1* double mutant phenotype was complemented by transformation with a *SAW2* genomic DNA fragment (see Methods). Nineteen out of 28 transformants showed a significant reduction in the number of leaf serrations (see Supplemental Figure 3 online). Since complementation of the mutant phenotype looks to be dosage dependent, both the number of copies inserted and the position of insertion may influence the extent of complementation in the transformant.

bel1 Does Not Affect the *saw1 saw2* Double Mutant Phenotype

Since BEL1 and the SAW proteins are very similar in structure, expression, and interaction pattern, a triple mutant was generated with *saw1-1*, *saw2-1*, and *bel1-1* to check for potential genetic redundancy or interaction. The progeny of an F2 plant that was homozygous for *saw1-1* and *saw2-1* and heterozygous for *bel1-1* (*bel1-1* is female sterile) were screened for triple mutants. The triple mutants identified showed an additive phenotype, including both *bel1-1*–like ovule defects and serrated leaves similar to those of the *saw1-1 saw2-1* double mutant, indicating that *BEL1* and *SAW* genes are not functionally redundant in tissues where their expression overlaps and/or as yet uncharacterized genes provide additional functional redundancy masking the affect of BEL1 loss.

SAW1 and the Class 1 *KNOX* Genes *STM*, *BP*, and *KNAT2* Are Expressed in the Shoot Apex in Nearly Mutually Exclusive Domains

As shown above, *SAW1* transcript in the shoot is found primarily in leafy organs and excluded from the meristematic region. Interestingly, although SAW1 has the ability to interact with Class 1 KNOX proteins STM, BP, and KNAT2, the available data for *STM*, *BP*, and *KNAT2* gene expression has shown that all three genes are expressed in meristems, stem, and reproductive organs but not leaves, sepals, and petals (Lincoln et al., 1994; Long et al., 1996; Pautot et al., 2001). To verify the nonoverlap in expression pattern, we used in situ hybridization to compare

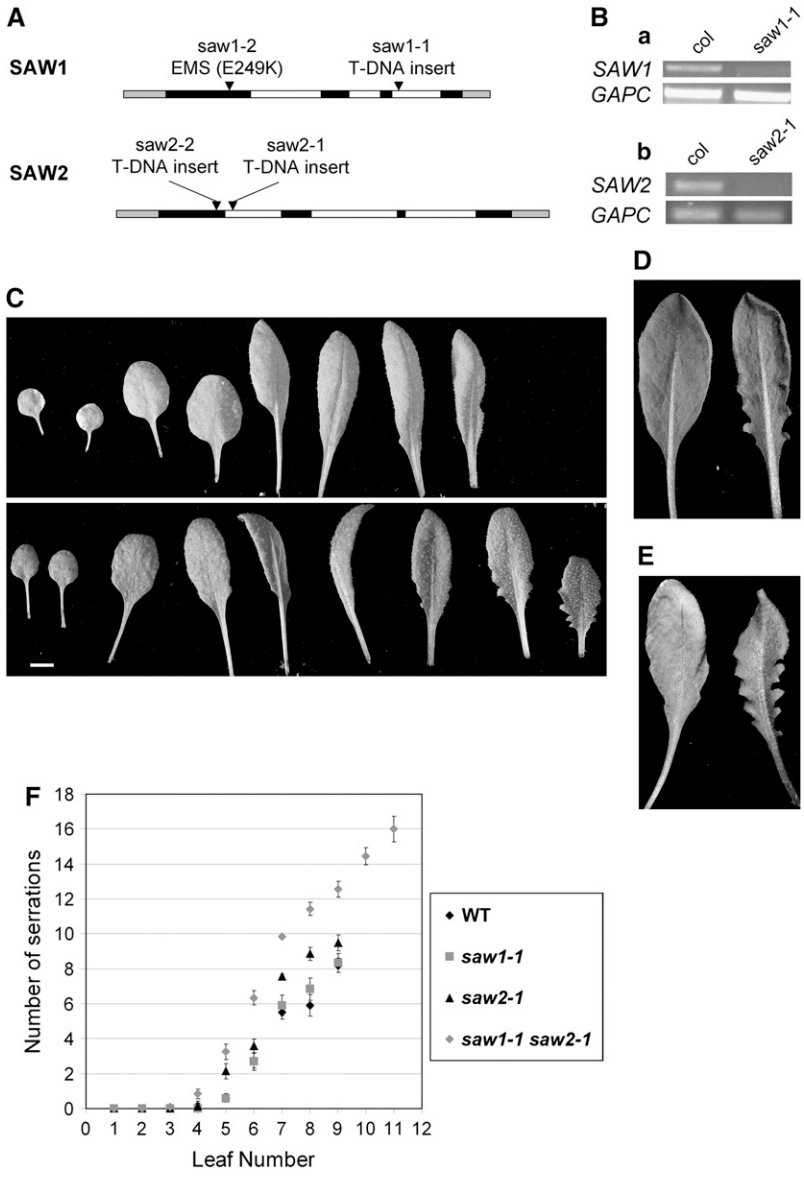

Figure 3. SAW Proteins Affect Leaf Margin Development.

(A) Graphical representations of the transcribed regions of *SAW1* and *SAW2* genes. Black, white, and gray boxes indicate exons, introns, and untranslated regions, respectively. The position of mutation/insertion in each mutant allele is marked by an arrowhead.

(B) RT-PCR analysis of *SAW1* and *SAW2* expression in wild-type (Col) and *saw* mutants. The fifth and sixth leaves were harvested from 4-week-old plants for RNA extraction and cDNA synthesis. (a) *SAW1* expression is considerably reduced in *saw1-1* compared with the wild type. Cytosolic-glyceraldehyde-3-phosphate dehydrogenase (*GAPC*) was used as a loading control. *SAW1*, 35 cycles; *GAPC*, 28 cycles. (b) There is no detectable *SAW2* expression in the leaves of saw2-1 mutants, but *SAW2* is detected in wild-type leaves. *SAW2*, 35 cycles; *GAPC*, 25 cycles.

(C) A comparison of the leaves of 4-week-old wild-type (top) and *saw1-1 saw2-1* (bottom). *saw1-1 saw2-1* double mutants had more serrations than the wild type from the seventh leaf onward. The fourth leaf of the double mutant was longer and more ovate than the fourth wild-type leaf.

(D) Leaf margins of *saw 1-1 saw2-1* double mutants are more revolute than wild-type leaf margins, as shown by an abaxial view of the eighth leaf of 4-week-old wild-type (left) and *saw1-1 saw2-1* (right) plants.

(E) The difference in the length of leaf serrations is more pronounced in older plants, as shown by an adaxial view of the ninth leaf of five-week-old wild-type (left) and *saw1-1 saw2-1* plants (right).

(F) Leaves of both *saw1-1 saw2-1* double mutants and *saw2-1* single mutants had more serrations than wild-type leaves. Scatterplot showing the number of serrations for each leaf of 5-week-old wild-type, *saw1-1*, *saw2-1*, and *saw1-1 saw2-1* plants. Serrations were counted only on the rosette leaves that had been initiated prior to bolting. Points represent means ± SE. As can be seen from the chart, *saw1-1 saw2-1* double mutants also initiate more leaves than the wild type prior to bolting.

Table 2. Serration Length and Flowering Time in Wild-Type and *saw* Mutants

	Average Serration Length (mm)	Days to Bolting	Number of Rosette Leaves at Bolting
Wild type	0.54 ± 0.039[a]	26.14 ± 0.27[a]	7.95 ± 0.19[a]
saw1-1	0.75 ± 0.074[a,b]	25.66 ± 0.2[a]	7.92 ± 0.27[a]
saw2-1	0.86 ± 0.071[b]	26.25 ± 0.45[a]	8.08 ± 0.2[a]
saw1-1 saw2-1	1.31 ± 0.073[c]	29.95 ± 0.35[b]	10.36 ± 0.22[b]

Values are mean ± SE ($n \geq 9$). The serrations were measured in the seventh leaf of 4-week-old plants. a, b, and c in each column denote significant differences (analysis of variance, P = 0.05). Means with the same letters are not significantly different.

SAW1 transcript distribution in the inflorescence with that for *STM* and *BP*. Our results (Figure 4A) clearly indicate that in these tissues, the *SAW1* transcript distribution is adjacent to but does not significantly overlap with that of either *STM* or *BP* except in the stage 1 to 2 floral meristem. These data suggest that interaction between SAW1 and Class 1 KNOX proteins in the developing inflorescence either does not occur, occurs at early stages only to resolve to mutually exclusive domains, or occurs in cells along the common border of the different expression domains.

BP Is Ectopically Expressed in the Leaves of *saw1 saw2* Double Mutants

The leaf serrations of the *saw1-1 saw2-1* double mutant are similar to those found in the leaves of *BP* overexpression lines with weak phenotypes (Chuck et al., 1996). *BP* expression is not detected in wild-type *Arabidopsis* leaves (Byrne et al., 2000). To test if there is a change in *BP* expression pattern in the *saw1-1 saw2-1* double mutants, we introduced a *BP:GUS* transgene (Ori et al., 2000) into a *saw1-1 saw2-1* double mutant background by crossing the appropriate lines and screening the F2 population. *BP:GUS* expression was detected in the hydathodes (present at the tip of serrations) of the *saw1-1 saw2-1* double mutants (Figure 4B) but not in the wild type. The intensity of GUS expression was roughly proportional to the size of the serration in the leaf margin (Figure 4B). *BP:GUS* expression was also observed in secondary serrations found in the ninth leaf and onwards (Figure 4B, d, arrow).

In addition to misexpression of *BP* in the leaf, 4-methylumbelliferyl β-D-glucuronide fluorometric assays (see Methods) revealed increased *BP:GUS* expression in the inflorescence and stem internodes of *saw1 saw2* double mutants (see Supplemental Figure 4 online), indicating that *BP* (and perhaps other KNOX genes) may be upregulated in areas where *SAW* and *BP* expression overlap.

To further characterize the interactions of SAW and BP, *saw1 saw2 bp* triple mutants were generated. These plants had the characteristics of both *saw1 saw2* double mutant (serrated leaves) and the *bp* phenotype (downward-pointing pedicels; see Supplemental Figure 6 online). The lack of a genetic interaction might be ascribed to the possible misexpression of other Class 1 *KNOX* genes, as was observed in the *as1* and *as2* mutants (Byrne et al., 2000; Ori et al., 2000).

In support, our RT-PCR data does indicate that besides *BP*, the *KNOX* genes *KNAT6* and *STM* are also expressed in the leaves of *saw1 saw2* but not in the wild type (see Supplemental Figure 7 online).

SAW1 and SAW2 Function in Parallel with AS1 to Regulate Leaf Margin Development

The *as1* mutant of *Arabidopsis* exhibits lobing of the leaves and misexpression of *KNOX* genes, such as *BP* (Tsukaya and Uchimiya, 1997; Byrne et al., 2000; Semiarti et al., 2001). Like the *saw1 saw2* double mutant serrations, the number of lobes in the *as1* mutant increases with the leaf number (Ori et al., 2000). To investigate the genetic interaction between *SAW1*, *SAW2*, and *AS1*, we constructed the *saw1 saw2 as1* triple mutant. The leaves (fifth leaf and higher) of *saw1-1 saw2-1 as1-1* triple mutants exhibited more lobing/serrations than *as1* and also showed deeper sinuses than either *as1* or the *saw1-1 saw2-1* double mutants (Figure 5). Although the triple mutant had more lobes than are found in *as1* single mutants, the lobes were fewer in number than the serrations found in *saw1-1 saw2-1* double mutants (Figure 5C). One possible explanation for this is that the *as1* mutant has fewer hydathodes than the wild type and hence is unable to make as many serrations/lobes (Tsukaya and Uchimiya, 1997). Another possibility is that the longer serrations are formed at the expense of the serration number. Such an inverse correlation between serration length and serration number has been observed in a comparison of different species of *Begonia* (Mclellan and Dengler, 1995). In any case, these additive phenotypic effects observed in the double mutant suggest that the functions regulated by SAW1 and SAW2 are relatively independent of those regulated by AS1. Furthermore, RT-PCR analysis of *SAW1* expression in wild-type and *as1* leaves indicates that there is no difference in expression (see Supplemental Figure 5 online). Therefore, *as1* phenotype is not a consequence of *SAW1* downregulation. Taken together, these data indicate that AS1 and SAW1 are likely functioning in parallel pathways to repress *BP* expression.

Ectopic Expression of *SAW1* Suppresses Shoot Growth

The *saw1-1 saw2-1* loss-of-function phenotype suggests that the *SAW* genes function, at least in part, to suppress growth in

Table 3. Serrations in the Seventh Leaf of Different Allele Combinations of *saw* Mutants

	Wild Type	*saw1-1 saw2-1*	*saw1-2 saw2-1*	*saw1-1 saw2-2*
Average number of serrations	5.5 ± 0.38[a]	9.8 ± 0.37[b]	9.7 ± 0.41[b]	10.2 ± 0.24[b]

Values are mean ± SE ($n = 12$). a and b denote significant differences (analysis of variance, P = 0.05). Means with the same letters are not significantly different.

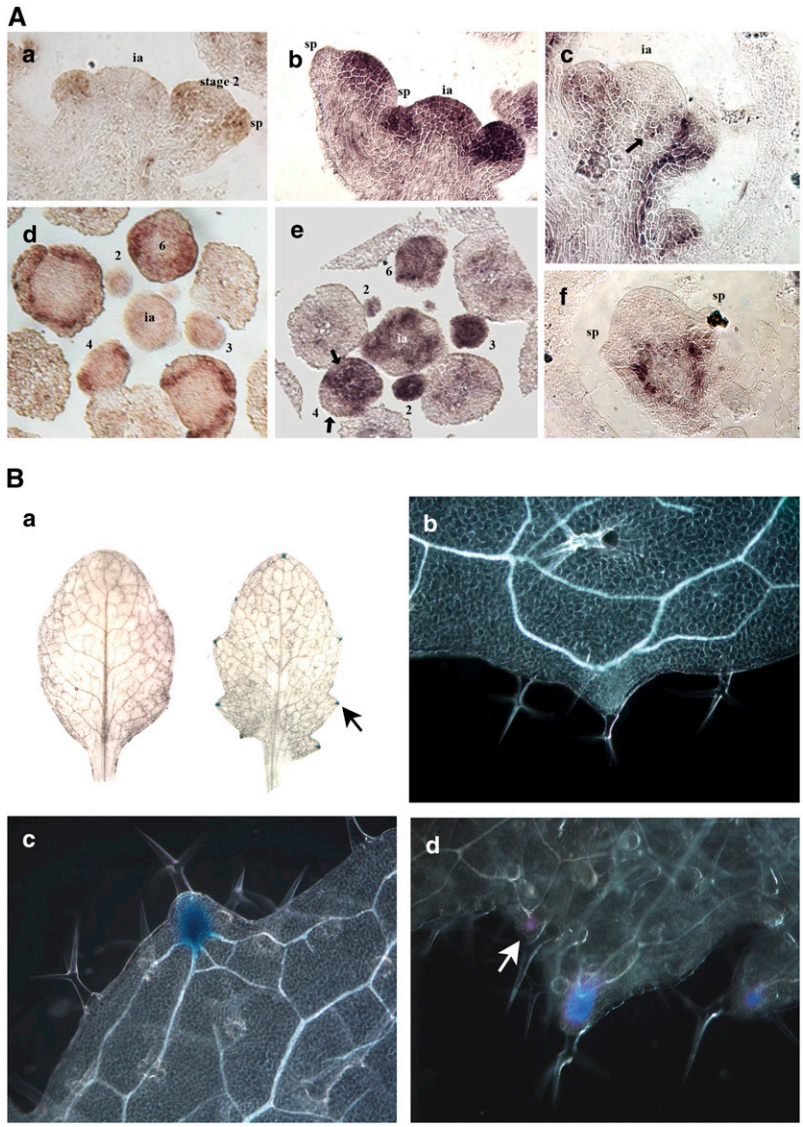

Figure 4. *SAW* Genes Suppress *BP* Expression in Leaves.

(A) In situ hybridization showing *SAW1*, *STM* and *BP* expression patterns. (a) and (d) Probed with *SAW1* antisense transcript. (b) and (e) Probed with *STM* antisense transcript. (c) and (f) Probed with *BP* antisense transcript. (a) to (c) Longitudinal sections; (d) and (e) transverse sections through an inflorescence apex. (f) Longitudinal section through a stage 3 flower. Numbers indicate the floral stages as described by Smyth et al. (1990). sp, sepal; ia, inflorescence apex.

(B) *BP* is misexpressed in leaves of *saw* double mutants. (a) Whole mounts of *BP:GUS* Col (left) and *BP:GUS saw1-1 saw2-1* (right) leaves assayed for GUS activity. Arrow points to the *BP:GUS* expression localized to the hydathodes. (b) and (c) Higher magnification dark-field image of (a). (b) *BP:GUS* Col and (c) *BP:GUS saw1-1 saw2-1*. (d) Dark-field image of a whole mount of the ninth leaf of a 4-week-old *BP:GUS saw1-1 saw2-1* plant assayed for GUS activity. Arrow points to *BP:GUS* expression in a secondary serration.

developing leaves. To test this hypothesis, transgenic plant lines expressing *SAW1* ectopically were generated by transforming *Arabidopsis* with a *SAW1* gene under the control of a tandem cauliflower mosaic virus 35S promoter. Of 100 transformants recovered, 15 showed a similar set of morphological defects described below. All aspects of the phenotype segregated together with the T-DNA, and RNA gel blot analysis showed such plants to have a much higher level of *SAW1* transcript than the wild type (see Supplemental Figure 9 online). Taken together, these data suggest that the phenotype is due to over/ectopic expression of *SAW1*.

The *35S:SAW1* shoots were significantly smaller than that of the wild type (Figure 6A). Leaves were rounder in shape and either flat or curved in the dorsal-ventral axis toward the adaxial side unlike wild-type leaves that are slightly curved toward the abaxial side (Figure 6A, c) or the *saw* mutant, which has revolute

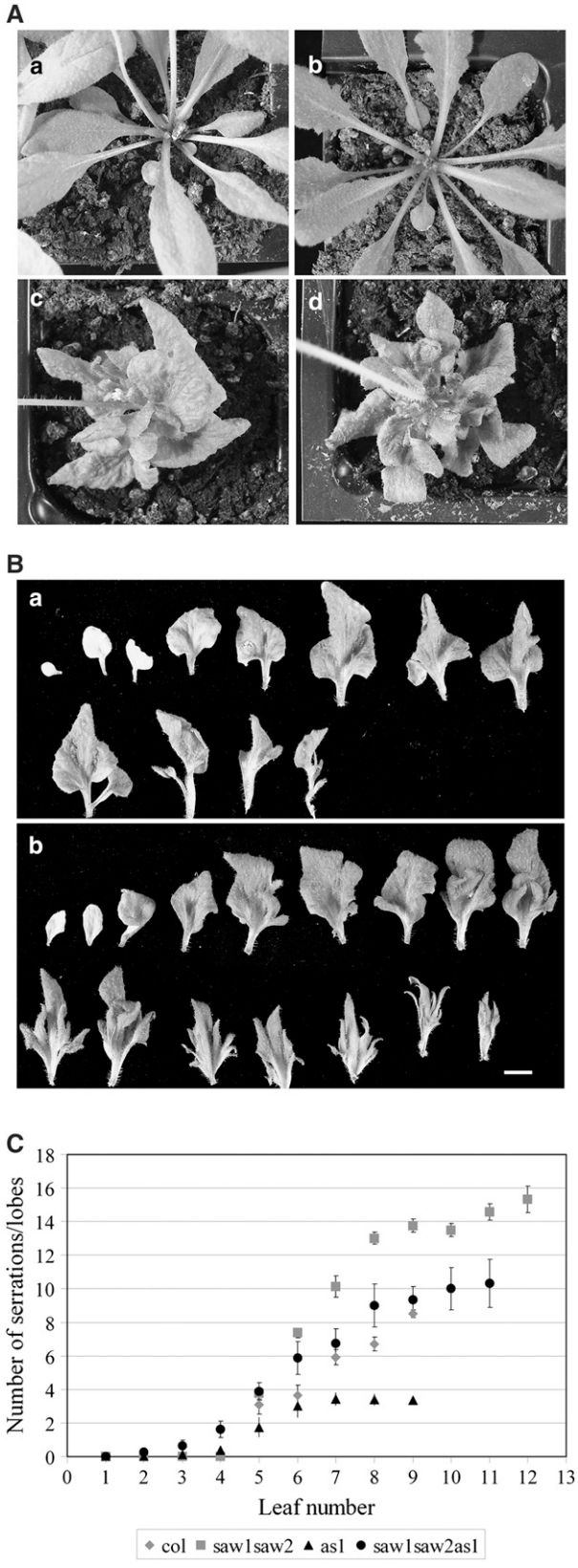

Figure 5. Phenotypes of *saw1-1 saw2-1 as1* Triple Mutants.

(A) Rosette leaves of 5-week-old plants. (a) The wild type, (b) *saw1-1 saw2-1*, (c) *as1*, and (d) *saw1-1 saw2-1 as1*. The inflorescence has been removed from (b).

(B) A comparison of the leaves of 6-week-old *as1* (top) and *saw1-1 saw2-1 as1* (bottom). The top row of each panel has the rosette leaves formed prior to bolting. The bottom row rosette leaves are the ones formed after bolting (marked by the presence of secondary inflorescences in their axils). Bar = 5 mm.

(C) Scatterplot showing the number of serrations for each leaf of 5-week-old wild-type (Col), *saw1-1 saw2-1*, *as1*, and *saw1-1 saw2-1 as1* plants. Serrations were counted only on the rosette leaves that had been initiated prior to bolting. Points represent means ± SE.

leaves (Figure 3D). These data suggest defects in the abaxial-adaxial polarity of *35S:SAW1*. Comparison of the cell types of the *35S:SAW1* abaxial and adaxial leaf surfaces with those of the wild type showed no obvious differences, indicating that the polarity defects were primarily due to differences in adaxial-abaxial growth rather than cell identity. Internodal length of the inflorescence stem was significantly shorter than the wild type, and measurements of stem epidermal cell length indicated that the growth defect was due to both a decrease in cell size and number (Figure 6A, d, Table 4).

The flowers of *35S:SAW1* plants also showed morphological defects (Figure 6B). The number of organs in the second and third whorls was consistently less than in the wild type (Figures 6B and 6C), and organ fusions were not uncommon (Figure 6B, e and f). These phenotypes are similar to those described for the weak *stm-2* allele, which also exhibits a reduction in organ number and organ fusions in the second and third whorls (Clark et al., 1996). Like the leaves, floral organs were smaller than the wild type. Petals were sometimes folded and pistils had an irregular bumpy appearance likely due to growth suppression in the silique valves (Figure 6B, c). Finally, *35S:SAW1* plants were sterile in part due to reduced pollen development in the anther and a decrease in stamen length that prevented self-fertilization. However, hand pollination of *35S:SAW1* pistils with their own pollen produced viable seed. Taken together, these data suggest that SAW1 can act as a negative regulator of growth throughout the plant.

35S:SAW1 Can Suppress the Leaf Phenotype of *as1* Mutants

As described earlier, the *as1* mutant shows lobed leaves that are associated with ectopic expression of Class 1 *KNOX* genes. Since the *SAW1* genes also suppress KNOX function in the leaf, we tested their ability to suppress the *as1* mutant phenotype when expressed ectopically. The leaf phenotype of *35S:SAW1 as1* plants more closely resembled that of *35S:SAW1* alone, suggesting that SAW1 function can partially complement the *as1* mutant phenotype (Figure 7A). To determine whether *35S:SAW1* has a direct effect on *BP* expression in *as1* leaves, RNA gel blot analysis was used to compare *BP* expression in leaves of *as1* and *35S:SAW1 as1* plants. *35S:SAW1* was sufficient to significantly repress *BP* expression in the leaves of *as1* mutants (Figure 7B). Since the level of expression of *SAW1* remained unchanged in an

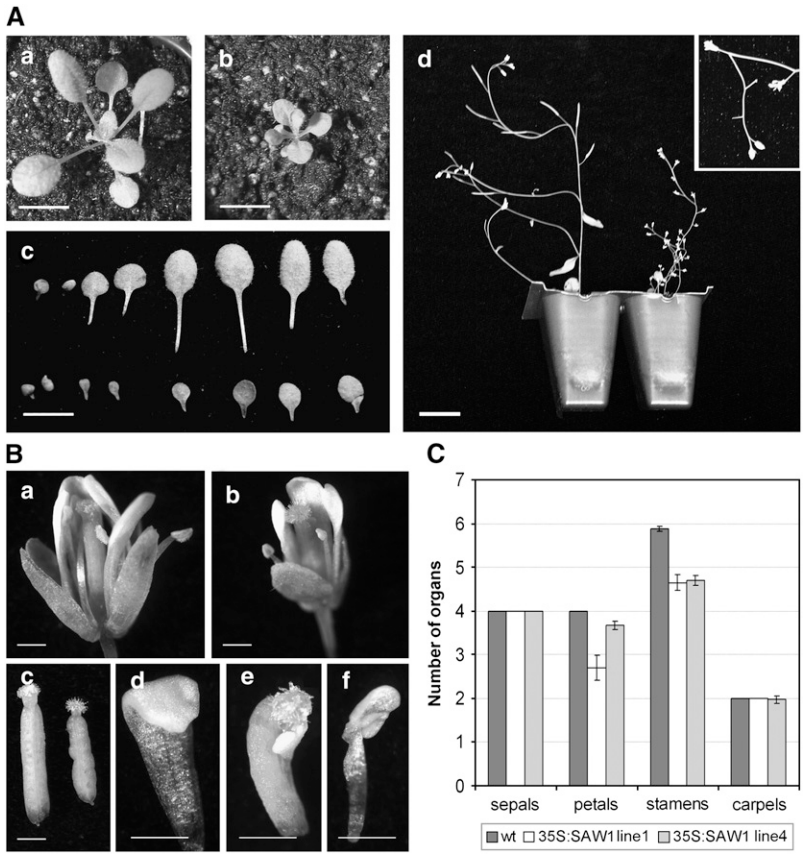

Figure 6. Phenotypes of *35S:SAW1*.

(A) Shoot morphology. (a) and (b) 2.5-week-old plants: the wild type (a) and 35S:SAW1 (b) (bars = 5 mm). (c) A comparison of the leaves of 3-week-old wild type (top) and *35S:SAW* (bar = 2 cm). (d) Four-week-old wild-type (left) and *35S:SAW1* (right) plants. Inset shows the fishbone-like growth defects observed in ~5% of the inflorescences (including coflorescences) (bar = 2 cm).

(B) Organ defects in *35S:SAW1* flowers. (a) and (b) Stage 13 flowers of wild-type and *35S:SAW1* plants. Note that there are only three petals in this *35S:SAW1* flower. (c) Gynoecia of stage 13 flowers of wild-type (left) and *35S:SAW1* plants (right). (d) to (f) Floral organ defects observed in some of the *35S:SAW1* flowers. (d) Petal showing distal folding. (e) Stamen-carpel fusion. (f) Petal-stamen fusion. Bars = 1 mm.

(C) Floral organ numbers in the wild type and *35S:SAW1*. Average number of sepals, petals, stamens, and carpels observed in the wild type and progeny of two independent transformed lines (lines 1 and 4). Error bars indicate SE.

as1 mutant (see Supplemental Figure 5 online), it is quite possible that in wild-type leaves, *AS1* and *SAW1* repress *BP* expression in leaves by independent mechanisms, possibly in temporally and/or spatially distinct subdomains of the leaf.

DISCUSSION

During plant morphogenesis, shape is achieved primarily by establishing domains of differential growth within the various plant organs. In the meristem and stem, BLH proteins BLR and PNF and Class 1 KNOX TALE homeodomain proteins BP and STM interact to positively regulate growth (Byrne et al., 2003; Smith and Hake, 2003; Bhatt et al., 2004; Kanrar et al., 2006). We have investigated the roles of two previously uncharacterized *Arabidopsis* BEL1-like TALE homeodomain genes, *SAW1* and *SAW2*. Unlike *BLR* and *PNF*, the *SAW* genes contribute to morphogenesis of the leaf and perhaps other organs as well by reducing growth in specific domains. This negative regulation of growth by SAW is correlated with an inhibition of *BP* gene expression, suggesting a mechanism for growth suppression through inhibition of *KNOX* gene expression. Therefore, the SAW proteins play a critical role in plant morphogenesis and one that is

Table 4. Cell Size and Number of Stem Epidermal Cells in the Wild Type and *35S:SAW1*

	Average Cell Length (mm)	Length of Internode (mm)	Estimated Number of Cells in One Internode
WT	0.25 ± 0.006[a]	18.9 ± 0.7[a]	74
35S:SAW1	0.14 ± 0.003[b]	8.5 ± 0.5[b]	64

Values are mean ± SE. a and b in each column denote significant differences (Student's *t* test, P = 0.05). Means with the same letters are not significantly different.

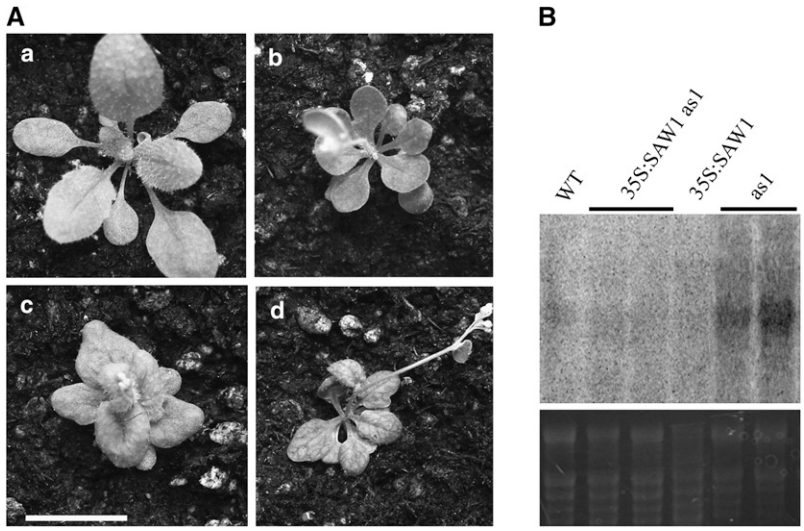

Figure 7. *35S:SAW1* Suppresses the *as1* Leaf Phenotype.

(A) Four-week-old plants. (a) The wild type, (b) *35S:SAW1*, (c) *as1*, and (d) *35S:SAW1 as1*. Bar = 10 mm.
(B) RNA gel blot showing *BP* expression in leaves. Ten micrograms of total RNA isolated from leaves was loaded and hybridized to a *BP*-specific probe. The bottom panel shows the ethidium bromide–stained gel (loading control).

in apparent direct opposition to their related homologs *BLR* and *PNF*.

SAW Proteins Are Negative Regulators of Growth

Loss- and gain-of-function mutant phenotypes suggest that a major role of *SAW1* and *SAW2* is to negatively regulate growth. *SAW1* and *SAW2* are expressed in the adaxial domain of the lateral organs early in development. *saw1 saw2* loss-of-function lines have revolute/downward curling margins, suggesting an increase in the adaxial-to-abaxial growth of the leaf. Conversely, *35S:SAW1* leaves are either flat or slightly curved toward the adaxial side, suggesting a decrease in adaxial-to-abaxial growth. In addition, *35S:SAW1* leaves were substantially reduced in overall size with a phenotype similar to plants overexpressing *ROTUNDIFOLIA4*, a gene that regulates polar cell proliferation in leaves (Narita et al., 2004). Taken together, these data suggest that SAW function limits growth on the adaxial side, where it is expressed early in leaf development, perhaps to promote curvature of the leaf over the meristem until leaf blade expansion.

SAW1 and *SAW2* are expressed in the hydathode regions of mature *Arabidopsis* leaves. Mild serrations occur naturally in wild-type *Arabidopsis* plants and typically occur at hydathodes, although a visible serration is not found at every hydathode (Tsukaya and Uchimiya, 1997; Candela et al., 1999). *saw* double mutants have increased numbers and sizes of serrations corresponding to the positions of the hydathodes in leaf margins of wild-type leaves, while *35S:SAW1* leaves have no obvious leaf serrations. These data suggest that one role of the SAW proteins is to limit growth at the hydathodes, thus limiting serration in the *Arabidopsis* leaf margin. That the serration could be due to increased growth at the hydathode is supported by the ectopic expression of the Class 1 *KNOX* gene *BP* at hydathodes in *saw1 saw2* double mutants (see also below).

In addition to the specific effects of SAW function on leaves, constitutive expression of *SAW1* appears to negatively regulate growth throughout the plant. The length and circumference of the stems and sizes of all lateral organs are reduced in *35S:SAW1* plants. *35S:SAW1* floral organ abnormalities involving a decrease in organ number and organ fusions suggest defects in maintaining appropriate growth within the meristem. It is noteworthy that a floral phenotype analogous to that of *35S:SAW1* observed in the weak *stm-2* mutant has been ascribed to the reduced size of the floral meristem in this mutant (Clark et al., 1996). Given that SAW proteins negatively regulate *BP* expression, *SAW1*, when ectopically expressed in the floral meristem, may also interfere with STM function, leading to *stm-2* like defects in floral patterning. Quantitative real-time PCR analysis of the expression of *KNOX* genes in the vegetative shoot apex did not reveal any significant reduction of expression in *35:SAW1* in comparison to the wild type (see Supplemental Figure 8 online). It is possible that the reduction of *KNOX* gene expression is localized, and this might be the reason why the disruption of meristem activity is not evident in all of the lateral organs.

Finally, *SAW1* and/or *SAW2* are expressed in a number of organs for which no obvious phenotype exists in the *saw1 saw2* double mutant. These organs include petals, cotyledons, stems, styles, and roots. Indeed, the observed leaf phenotypes themselves are more subtle than the leaf expression pattern suggested. It is possible that redundancy with other BLH genes obscures SAW function in these organs. Alternatively, it is possible that both *saw1* alleles obtained for this study are hypomorphic, and a stronger allele could have additional phenotypes. Thus, determination of the roles of the *SAW* genes in these organs awaits further genetic analysis.

SAW Is a Negative Regulator of *BP*

Several lines of evidence indicate that SAW proteins act at least in part by negatively regulating *BP*. First, *BP* is misexpressed in *saw* leaves at the regions marked by hydathodes (Figure 4B). Second, *35S:SAW1* is able to reverse the BP-associated leaf lobing observed in *as1* mutants and decrease ectopic *BP* expression in *as1* leaves (Figure 7). Third, *SAW1* and *SAW2* are expressed in dorsiventrally flattened organs, such as leaf and sepal, while *BP* and *STM* are excluded from these organs (Figures 2 and 3A). *Arabidopsis* BP protein has been associated with the promotion of growth. Loss of BP function in *bp* mutant plants results in a shortened inflorescence shoot and pedicels (Douglas et al., 2002; Venglat et al., 2002), indicating that BP is involved in proper elongation of stems. *Arabidopsis* plants transformed with *35S:BP* exhibit leaf phenotypes of increased serrations and/or lobing as well as the establishment of ectopic meristems in the leaf margins (Lincoln et al., 1994; Chuck et al., 1996). Indeed, some of the weaker *35S:BP* lines resemble *saw1 saw2* mutants, suggesting that the ectopic expression of *BP* in the *saw* mutants may be sufficient to cause serration. However, the domain of *BP* expression in *saw1 saw2* suggests a mechanism of serration growth under the region of expression in the leaf margin rather than a repression of growth in the sinuses, as observed in the 35S:BP plants (Lincoln et al., 1994; Chuck et al., 1996; Hay et al., 2003). Interestingly, a positive correlation between serration length and the size of the *BP* expression domain in the *saw1 saw2* leaves is observed (Figure 4B, d). A more detailed analysis would be required to clarify this point. Nonetheless, it is possible that the SAW proteins regulate growth by suppressing *KNOX* expression in specific domains of lateral organs. In the absence of SAW function, localized *BP* expression might promote growth in regions below the site of expression, resulting in serrated, revolute leaves.

Interestingly, an STM-like protein in *Cardamine hirsuta* promotes compound leaf formation in wild-type plants by prolonging the duration of cell division in specific regions of the leaf primordia (Hay and Tsiantis, 2006). Since STM is closely related to BP, it is possible that BP-mediated cell divisions are the cause of leaf phenotypes in *saw* mutants. Alternatively, *BP* expression might be establishing a meristematic region where *STM* and other Class 1 *KNOX* genes are expressed. Since our RT-PCR results indicate STM misexpression in the leaves of *saw* mutants (see Supplemental Figure 7 online), either of these mechanisms may exist in the *saw* mutants.

The microRNA *miR164A* has been shown to regulate the extent of serration by regulating the levels of CUP-SHAPED COTYLEDON (CUC2) in the leaf sinuses (Nikovics et al., 2006). Absence of *miR164A*-mediated reduction of CUC2 transcripts results in increased leaf serrations, suggesting that CUC2 is possibly repressing growth in the sinuses, resulting in increased depths of serrations (Nikovics et al., 2006). It will be interesting to see if the *CUC2* levels are changed in the *saw1 saw2* mutants.

As observed for the *saw1 saw2* double mutant, the *BP* gene is misexpressed in the leaves of the *as1* mutant (Ori et al., 2000; Semiarti et al., 2001). AS1 is a MYB domain–containing transcriptional factor required for normal leaf development. *as1* mutants have leaves with irregular lobed blades (Tsukaya and Uchimiya, 1997). This phenotype has been correlated with the misexpression of multiple Class 1 *KNOX* genes in the leaves (Byrne et al., 2000; Ori et al., 2000). Therefore, like SAW1 and SAW2, AS1 appears to establish a boundary between the meristem and the leaves in part by repressing expression of KNOX genes in the developing leaves. These data suggest that the functions of SAW and AS1 are related. Ectopic/overexpression of *35S:SAW1* is able to partially suppress the *as1* mutant phenotype, and we found no evidence that one regulates the expression of the other, suggesting that SAW and AS1 function independently to repress expression of *KNOX* genes. However, the distinct phenotypes of the *as1* single and *saw1 saw2* double mutant and the additive effects observed in the *saw1 saw2 as1* triple mutants suggest that AS1 and SAW functions are not identical. SAW and AS1 may be functioning in temporally/spatially separated domains in the leaf and/or might have distinct target gene sets.

AS1 works in the same regulatory pathway as AS2, a Leu zipper–containing protein (Byrne et al., 2002; Iwakawa et al., 2002; Xu et al., 2003). *as2* mutants have phenotypes similar to those of *as1* and also suppress *KNOX* gene expression in the leaf (Serrano-Cartagena et al., 1999; Semiarti et al., 2001). Therefore, it is likely that *saw1 saw2 as2* interactions would be similar to those observed in *saw1 saw2 as1* triple mutants.

SAW and KNOX Interactions

BLH and KNOX proteins are DNA binding transcription factors. Protein–protein interactions amongst members of the BLH and KNOX families have been well documented (Bellaoui et al., 2001; Muller et al., 2001; Smith et al., 2002; Smith and Hake, 2003; Hackbusch et al., 2005). Several lines of evidence suggest that heterodimerization amongst members of these families is required for DNA binding and nuclear localization (Bhatt et al., 2004; Cole et al., 2006). As described earlier, BP and the BLH protein BLR/PNY/RPL/VAN interact to positively regulate inflorescence growth (Smith and Hake, 2003; Bhatt et al., 2004). Similarly, BLR/PNY/RPL/VAN and the paralogous protein PNF positively interact with STM to regulate meristem function (Byrne et al., 2003; Kanrar et al., 2006). For the SAW proteins, it has been shown that both SAW1 and SAW2 interact with BP in yeast two-hybrid assays (Figure 1B; Hackbusch et al., 2005). However, genetic and molecular analyses have revealed that the SAW proteins negatively regulate *BP* expression and function (Figures 4B and 7). Furthermore, *SAW* and *BP* are mostly expressed in mutually exclusive domains (Figure 4A). These findings raise the question of what functions SAW–BP interactions could have. Based on our data, we hypothesize that SAW and BP interactions are required for negative regulation of BP function. Mechanistically, such negative regulation could occur if the SAW-BP heterodimer acts as a repressor of *BP* expression. Alternatively, the regulation might be a result of BP being sequestered by SAW proteins and hence unable to interact with BLR/PNY/VAN and PNF proteins. In the latter case, it must be assumed that BLR-BP complexes are activators of BP expression. Thus, the titers of competing BLH proteins in a given cell and/or tissue might decide the fate of BP-derived functions in the tissue. KNOX proteins have been shown to move across cell layers in the

meristem (Kim et al., 2003, 2005). Long-range transport of KNOX transcripts via the phloem has also been reported (Kim et al., 2001, 2005). SAW proteins might repress the function of KNOX proteins trafficked into an inappropriate domain.

The fact that *BP:GUS* expression in stems of *saw* double mutants is more than double that found in wild-type stems suggests that SAW1 negatively regulates *BP* in some domain of the stem as well. However, unlike in leaves, *BP*, *SAW1*, and *SAW2* are expressed in overlapping domains in the stem cortex (Venglat et al., 2002; R. Kumar and G.W. Haughn unpublished results). Further studies are required to clarify the role of any of the SAW proteins in the stem and its relationship with BP function.

Conservation of SAW Function in Dicotyledonous Plants

In this report, we have shown that *SAW1* overexpression results in reduced organ size and flattened leaves. MDH1 (for *Malus domestica* Homeodomain protein 1) is a SAW1 ortholog from apple that shows higher amino acid sequence similarity to SAW1/SAW2 than to any other *Arabidopsis* BLH protein. Overexpression of *MDH1* in *Arabidopsis* resulted in phenotypes (Dong et al., 2000) strikingly similar to the ones observed in the *35S:SAW1* plants. This suggests that SAW1 function is conserved in dicotyledonous plants and may represent a common regulatory mechanism of differential organ growth in dicots.

Redundancy between *BEL1* and *SAW* Genes

The SAW proteins are most similar (in amino acid sequence) to the BEL1 protein, have overlapping expression patterns, and interact with a similar set of KNOX proteins. Moreover, the *bel1* mutant phenotype can be complemented by *35S:SAW1* (Figure 1C). However, *saw1 saw2 bel1* triple mutants have an additive phenotype. It is possible that there could be other BLH proteins that mask any functions common to SAW1, SAW2, and BEL1. Alternatively, it is also possible that BEL1 has diverged sufficiently from SAW1 and SAW2 to retain its ovule function but lost those needed for other tissues. In support of the latter hypothesis, we have found that unlike *35S:SAW1* plants, *35S:BEL1* does not have any observable changes outside the ovule (S.R. Hepworth and G.W. Haughn, unpublished results). A more complete understanding of BEL1 function outside the ovule must therefore await further analysis.

METHODS

Plant Materials and Growth Conditions

The *Arabidopsis thaliana* ecotypes Columbia-0 (Col-0), Col-2, Col with *erecta* mutation (Col er105), and Landsberg *erecta* were used as wild-type controls in phenotypic screens and other experiments for the mutants and transgenics, in accordance with their genetic backgrounds. *BP:GUS* was a gift from Sarah Hake (Ori et al., 2000). All Salk insertion lines, TILLING lines, and the *as1-1* mutant were ordered from the ABRC (stock numbers: *as1*, CS3374; *saw1*, SALK_009120; *saw1-2*, CS87673; *saw2-1*, SALK_121117; and *saw2-2*, SALK_149402). The genotypes of the *saw1* and *saw2* mutants and any double mutants generated were confirmed by PCR-based genotyping. Plants were grown as previously described (Bellaoui et al., 2001; Hepworth et al., 2005) and transformed using the *Agrobacterium tumefaciens*–mediated floral dip method (Clough and Bent, 1998).

Sequence Analysis

The amino acid sequences for the BLH proteins were aligned using the ClustalX program (Thompson et al., 1994, 1997) with default alignment parameters except for the protein matrix, for which BLOSUM62 (Henikoff and Henikoff, 1992) was used. To construct the phylogram based on the maximum likelihood method (Felsenstein, 1981), the aligned sequences were imported into Bioedit for manual editing (Hall, 1999; http://www.mbio.ncsu.edu/BioEdit/bioedit.html). Three highly conserved regions were identified (see Supplemental Figure 1A online), and these regions were selected for further analysis. The alignment of the conserved sequences was bootstrapped 1000 times using SEQBOOT (from PHYLIP version 3.6, distributed by J. Felsenstein, University of Washington, Seattle). The program Phyml (Guindon and Gascuel, 2003; Guindon et al., 2005) was then used to generate maximum likelihood–based trees for both bootstrapped and nonbootstrapped data sets. The trees were visualized using Treeview (R. Page; http://taxonomy.zoology.gla.ac.uk/rod/treeview.html) and processed with IrfanView (I. Skiljan; http://www.irfanview.com/) and Photoshop (Adobe Systems), where the bootstrap values were converted to 100 and added to the tree branches.

RT-PCR and Quantitative Real-Time PCR

cDNA was synthesized by RT using Superscript II RT (Invitrogen) and 1 μg of total RNA isolated from required organs of the mutants or the wild type. PCR was performed using 1 μL of cDNA as template and Taq DNA polymerase (Invitrogen) according to the manufacturer's instructions. Primers were as follows: BEL1, p1 5′-CACAAGTCACCACAGCAACA-3′/p2 5′-TGCTTGAATCTGTCCCACAA-3′; SAW1, p1 5′-CAGCGGGAATCTCTTCTTCC-3′/p2 5′-TGGATTTTGTGCTCTTGTCG-3′; SAW2, p1 5′-CCATTGGAGGGATCTACACG-3′/p2 5′-ATCCCCTAGAAGCTCACAGC-3′; BP, p1 5′-CGATGTTGAAGCCATGAAGG-3′/p2 5′-GCTGTTGTCGAGCCTCAAAG-3′; KNAT2, p1 5′-CGCGTATTCGAAAAGCTGAG-3′/p2 5′-CATGGTTCTCTCGCTGAATCTC-3′; KNAT6, p1 5′-AAATCGCTTGTCATCCTTCG-3′/p2 5′-TCACTCTCCCGTTGAATCTCC-3′; STM, p1 5′-CAACCCTTGCTCCTCTTCC-3′/p2 5′-CCTGTTGGTCCCATAGATGC-3′. Either GAPC (Western et al., 2004) or ACTIN8 (An et al., 1996) was used as a loading control. These genes were amplified using the following primer pairs: GAPC p1 5′-TGGGGAGACATTCTTGCTG-3′/p2 5′-GATGGGCTTGTGTGTGTTTG-3′; ACT8 p1 5′-TGTGACAATGGTACTGGAATGG-3′/p2 5′-TTGGATTGTGCTTCATCACC-3′. All PCR reactions were repeated at least three times, and the PCR cycle numbers were adjusted to ensure that the amplification was in the logarithmic phase. The PCR products were resolved in a 1% agarose gel and stained with ethidium bromide. Quantitative real-time PCR was performed in the MJ MinipOticon real-time PCR system (Bio-Rad Laboratories) using iQ SYBR Green Supermix (Bio-Rad Laboratories). Each real-time PCR experiment was done in triplicate, and the graph was generated from the pooled data of two independent experiments.

GUS Analysis

Generation of Promoter:GUS Constructs

For all constructs made during this project, PCR fragments were amplified using Expand High-Fidelity polymerase (Roche; according to the manufacturer's protocol) from Col-2 genomic DNA isolated as described (Dellaporta et al., 1983). For the promoter-GUS constructs, the promoter regions of *BEL1*, *SAW1*, and *SAW2*, including the 5′ untranslated region, were amplified using the following gene-specific primers: *BEL1*, p1

5′-GAATTCCAATCTCTTTCACGTACTGTGCG-3′/p2 5′-GGATCCTGTC-TCTCAAGAATTGAAAACCC-3′; *SAW1*, p1 5′-TTAGTCGACAAAGATTC-CCACATGGTGTC-3′/p2 5′-TATCTCGAGGTTATTCCCATATCAATACT-TCAATC-3′; *SAW2*, p1 5′-ATTATGAATTCTTGCAACCACCATTGAA-GAG-3′/p2 5′-ATTATCTCGAGCAAAGCTCTTGGATCCTGTAAG-3′. The *BEL1* promoter was cloned into pCR 2.1 blunt (Invitrogen) and then introduced into pBAR1 (a gift from Ben Holt and Doug Boyes, Dangl Lab, University of North Carolina) containing *GUS* that we subcloned from pBI101 (Clontech Laboratories). *SAW1* and *SAW2* promoters were cloned into pENTR1A (Invitrogen) and then subcloned into pGWB3 (a gift from Tsuyoshi Nakagawa, Research Institute of Molecular Genetics, Shimane University, Japan) by the Gateway LR recombination reaction (Invitrogen) according to the manufacturer's directions.

GUS Histochemical Assay

GUS histochemical assays were done on freshly isolated plant organs or whole seedlings using a protocol that was adapted for staining *Arabidopsis* (Sieburth and Meyerowitz, 1997). For whole mounts, stained tissues were destained by incubation in 70% ethanol overnight at room temperature. The destained samples were either directly viewed under a light microscope (Zeiss Axioskop microscope) or incubated in clearing solution (chloral hydrate:glycerol:water, 9:1:3 [w:v:v]; Mattsson et al., 2003) for 1 h to 4 d depending on the organ being cleared (ovules start clearing within an hour and leaves take 2 to 4 d) and photographed under the compound microscope or dissecting photomicroscope.

For resin embedding and sectioning, the stained samples were fixed with 3% glutaraldehyde (Canemco) in 0.5 M sodium phosphate buffer at 4°C overnight and then dehydrated through an ethanol series and embedded in Technovit 8100 resin based on the manufacturer's instructions (Heraeus Kulzer; Electron Microscopy Sciences, distributor). Embedded tissue was sectioned using a glass microtome. Sections were spread on glass slides and mounted with Entellan (Merck). The samples were then visualized under a light microscope and photographed using a SPOT digital camera (Diagnostic Instruments). The photographs were processed using Adobe Photoshop (Adobe Systems).

GUS Fluorometric Assay

GUS activity was quantified in crude protein extracts from stem internodes (the first two internodes from the base) and inflorescence apices (including the region from inflorescence meristem to the first open flower) from 5-week-old wild-type (Col-0), *BP:GUS* Col-0, and *BP:GUS saw1 saw2* plants using the 4-methylumbelliferyl β-D-glucuronide fluorometric assay (Jefferson et al., 1987). Protein concentrations were quantified against a BSA standard curve using the Bio-Rad protein microassay according to the manufacturer's instructions. The concentration of the hydrolysis product, 4-methylumbelliferone (MU), in each aliquot was measured using a Finstruments Fluoroskan plate reader (Thermo Electron/Labsystems; excitation at 365 ± 7 nm; emission at 460 ± 15 nm) at 0 h, 30 min, and 1 h and reported as absolute fluorescence units. The amount of MU produced by each sample was determined in comparison with an MU standard curve.

Complementation of *saw1 saw2* with a SAW2 Genomic Fragment

Expand high-fidelity polymerase (Roche) was used to amplify a wild-type genomic fragment containing the *SAW2* coding sequence (including introns), as well as 3000 kb of the 5′ and 1000 kb of the 3′ sequence, using the primers 5′-TTCGCGGCCGCTGCTATTTCAAGGACGTGAGC-3′ and 5′-CTAGCGGCCGCATTGTGACTTATTGGCGCTTTCC-3′. Genomic DNA isolated by the method of Dellaporta et al. (1983) from leaves of wild-type plants was used as a template for PCR. The PCR-generated fragment was cloned directly into the *Not*I site of the pART27 binary vector (Gleave, 1992). This construct was used to transform it into *saw1 saw2* double mutant plants. We then evaluated selected transformants for complementation of the mutant phenotypes.

Yeast Two-Hybrid Assays

A GAL4-based yeast two-hybrid system was used as described previously (Kohalmi et al., 1988). Plasmid constructs were generated by cloning full-length cDNAs into either the GAL4 DNA binding domain (DB) plasmid pBI-770 as the bait or the GAL4 transcriptional activation domain (TA) plasmid pBI-771 as the prey. Full-length *SAW1* and *BLH1* cDNAs were amplified from plasmids (obtained by screening flower-specific cDNA libraries) using the Expand high-fidelity PCR system (Invitrogen). The PCR product was digested with *Sal*I and *Not*I and cloned into pBI-771 to create TA-SAW1 and TA-BLH1. Construction of TA-BEL1, all the DB-KNOX, and DB-Cruciferin has been described earlier (Bellaoui et al., 2001). The bait and prey constructs were transformed into the yeast strain YPB2 (Fields and Song, 1989), and interacting transformants were selected on medium lacking Leu, Trp, and His. The interactions were further visualized using X-Gal filter assays that were performed as described previously (Kohalmi et al., 1988).

In Situ Hybridization Analysis

Tissue fixation, sectioning, hybridization, and signal detection were performed as described previously (Samach et al., 1997). Full-length *SAW1* cDNA was amplified from the TA-SAW1 construct (described earlier) and was used for probe preparation. Sections were viewed through a light microscope (Zeiss Axioskop II) and photographed under bright-field conditions using a SPOT digital camera (Diagnostic Instruments).

RNA Gel Blot Analysis

Approximately 10 μg of RNA isolated from leaves of *as1*, *35S:SAW1*, and *35S:SAW1 as1* plants was resolved in a denaturing agarose gel and blotted onto a nylon membrane as previously described (Western et al., 2004). The membrane was then hybridized with a ^{32}P-labeled *BP* probe and detected as previously described (Western et al., 2004), and the specific signal was detected with a Storm 860 PhosphorImager (Molecular Dynamics).

The *35S:SAW1* Construct

Full-length SAW1 cDNA was amplified by PCR from wild-type cDNA using the primers 5′-GCCTCTAGATGGAATAACTAAAACTTC-3′ and 5′-GCTCTAGACTAAAACCCCCAAACTC-3′. The resulting fragment was cut with *Xba*I and cloned into pGPTV pBAR (Becker et al., 1992) with a tandem 35S promoter with an AMV leader sequence (M. Bellaoui and G.W. Haughn, unpublished results) and transformed into Col-2 plants as described earlier.

Characterization of Mutant Phenotypes

All macroscopic images were either taken using a Nikon CoolPix camera or were scanned using an HP Scanjet 7400c (Hewlett Packard). Micrographs were taken using a dissection or compound microscope equipped with a Spot digital camera and Northern Eclipse software. Adobe Photoshop was used for image processing and the creation of montages.

To measure lengths of leaf serrations, leaves were scanned using a Canoscan 8400DF scanner (Canon). Scanned images were converted to gray scale, and threshold was adjusted to include only the leaves. Measurements were made using ImageJ software (National Institutes of Health; http://rsb.info.nih.gov/ij/) calibrated with a scanned ruler.

To evaluate cells of the *35S:SAW1* plants, epidermis was peeled from the bottom three internodes of stems of 5-week-old plants and mounted in 50% glycerol on glass slides. Cell counts and measurements were made using phase contrast optics of a compound light microscope.

Accession Numbers

The GenBank accession numbers and Arabidopsis Genome Initiative (AGI) locus identifiers of the *SAW* genes are as follows: *BLH2*/*SAW1*, AF173816 (GenBank), At4g36870 (AGI locus); *BLH4*/*SAW2*, AF353092 (GenBank), At2g23760 (AGI locus).

Supplemental Data

The following materials are available in the online version of this article.

Supplemental Figure 1. Sequence Conservation and Duplication in the BLH Proteins.

Supplemental Figure 2. RT-PCR Analysis of *BEL1*, *SAW1*, and *SAW2*.

Supplemental Figure 3. Complementation of *saw1 saw2* Double Mutants by a *SAW2* Genomic DNA Fragment.

Supplemental Figure 4. Increased *BP:GUS* Activity in Stems of *saw1 saw2* Double Mutants.

Supplemental Figure 5. RT-PCR Analysis of *SAW1*.

Supplemental Figure 6. The *saw1 saw2 bp* Triple Mutant Phenotype.

Supplemental Figure 7. RT-PCR Analysis of Class 1 *KNOX* Gene Expression.

Supplemental Figure 8. Real-Time PCR Analysis of Class1 *KNOX* Genes.

Supplemental Figure 9. RNA Gel Blot Comparing *SAW1* Expression in Wild-Type and *35S:SAW1* Plants.

ACKNOWLEDGMENTS

We thank the Seattle TILLING Project for screening for *saw1* mutants, the Salk Institute Genome Analysis Laboratory for T-DNA insertional lines, the ABRC at Ohio State University for providing us with the mutant seeds, Sarah Hake for the *BP:GUS* (*KNAT1:GUS*) line, Jeff Dangl for the pBAR1 plasmid, and Tsuyoshi Nakagawa for pGWB3 plasmid. We also thank Dmitry Belostotsky for providing necessary resources for the *saw1 saw2 bp* triple mutant screens, Tanya Hooker for critical reading of this manuscript, Juan Saldarriaga for comments on phylogenetic analysis, and Jin-Gui Chen for allowing us to use his MiniOpticon real-time PCR system. This work was supported by a Natural Sciences and Engineering Research Council (NSERC) Discovery grant to G.W.H., by NSERC postgraduate fellowships to M.S.P., and by a University of British Columbia Graduate Fellowship to R.K. and M.S.P.

Received November 10, 2006; revised August 6, 2007; accepted August 20, 2007; published September 14, 2007.

REFERENCES

Alonso, J.M., et al. (2003). Genome-wide insertional mutagenesis of *Arabidopsis thaliana*. Science **301:** 653–657.

An, Y.Q., McDowell, J.M., Huang, S.R., McKinney, E.C., Chambliss, S., and Meagher, R.B. (1996). Strong, constitutive expression of the Arabidopsis ACT2/ACT8 actin subclass in vegetative tissues. Plant J. **10:** 107–121.

Bao, X., Franks, R.G., Levin, J.Z., and Liu, Z. (2004). Repression of AGAMOUS by BELLRINGER in floral and inflorescence meristems. Plant Cell **16:** 1478–1489.

Barton, M.K., and Poethig, R.S. (1993). Formation of the shoot apical meristem in *Arabidopsis thaliana*: An analysis of development in the wild type and in the shoot meristemless mutant. Development **119:** 823–831.

Becker, A., Bey, M., Burglin, T.R., Saedler, H., and Theissen, G. (2002). Ancestry and diversity of BEL1-like homeobox genes revealed by gymnosperm (*Gnetum gnemon*) homologs. Dev. Genes Evol. **212:** 452–457.

Becker, D., Kemper, E., Schell, J., and Masterson, R. (1992). New plant binary vectors with selectable markers located proximal to the left T-DNA border. Plant Mol. Biol. **20:** 1195–1197.

Bellaoui, M., Pidkowich, M.S., Samach, A., Kushalappa, K., Kohalmi, S.E., Modrusan, Z., Crosby, W.L., and Haughn, G.W. (2001). The Arabidopsis BELL1 and KNOX TALE homeodomain proteins interact through a domain conserved between plants and animals. Plant Cell **13:** 2455–2470.

Bhatt, A.M., Etchells, J.P., Canales, C., Lagodienko, A., and Dickinson, H. (2004). VAAMANA–a BEL1-like homeodomain protein, interacts with KNOX proteins BP and STM and regulates inflorescence stem growth in Arabidopsis. Gene **328:** 103–111.

Blanc, G., Hokamp, K., and Wolfe, K.H. (2003). A recent polyploidy superimposed on older large-scale duplications in the Arabidopsis genome. Genome Res. **13:** 137–144.

Byrne, M.E., Barley, R., Curtis, M., Arroyo, J.M., Dunham, M., Hudson, A., and Martienssen, R.A. (2000). Asymmetric leaves1 mediates leaf patterning and stem cell function in Arabidopsis. Nature **408:** 967–971.

Byrne, M.E., Groover, A.T., Fontana, J.R., and Martienssen, R.A. (2003). Phyllotactic pattern and stem cell fate are determined by the Arabidopsis homeobox gene BELLRINGER. Development **130:** 3941–3950.

Byrne, M.E., Simorowski, J., and Martienssen, R.A. (2002). ASYMMETRIC LEAVES1 reveals knox gene redundancy in Arabidopsis. Development **129:** 1957–1965.

Candela, H., Martinez-Laborda, A., and Micol, J.L. (1999). Venation pattern formation in *Arabidopsis thaliana* vegetative leaves. Dev. Biol. **205:** 205–216.

Chen, H., Rosin, F.M., Prat, S., and Hannapel, D.J. (2003). Interacting transcription factors from the three-amino acid loop extension superclass regulate tuber formation. Plant Physiol. **132:** 1391–1404.

Chuck, G., Lincoln, C., and Hake, S. (1996). KNAT1 induces lobed leaves with ectopic meristems when overexpressed in Arabidopsis. Plant Cell **8:** 1277–1289.

Clark, S.E., Jacobsen, S.E., Levin, J.Z., and Meyerowitz, E.M. (1996). The CLAVATA and SHOOT MERISTEMLESS loci competitively regulate meristem activity in Arabidopsis. Development **122:** 1567–1575.

Clough, S.J., and Bent, A.F. (1998). Floral dip: A simplified method for Agrobacterium-mediated transformation of *Arabidopsis thaliana*. Plant J. **16:** 735–743.

Colbert, T., Till, B.J., Tompa, R., Reynolds, S., Steine, M.N., Yeung, A.T., McCallum, C.M., Comai, L., and Henikoff, S. (2001). High-throughput screening for induced point mutations. Plant Physiol. **126:** 480–484.

Cole, M., Nolte, C., and Werr, W. (2006). Nuclear import of the transcription factor SHOOT MERISTEMLESS depends on heterodimerization with BLH proteins expressed in discrete sub-domains of the shoot apical meristem of *Arabidopsis thaliana*. Nucleic Acids Res. **34:** 1281–1292.

Dellaporta, S.L., Wood, J., and Hicks, J.B. (1983). A plant DNA minipreparation: Version II. Plant Mol. Biol. Rep. **1:** 19–21.

Dong, Y.H., Yao, J.L., Atkinson, R.G., Putterill, J.J., Morris, B.A., and Gardner, R.C. (2000). MDH1: An apple homeobox gene belonging to the BEL1 family. Plant Mol. Biol. **42:** 623–633.

Douglas, S.J., Chuck, G., Dengler, R.E., Pelecanda, L., and Riggs, C.D. (2002). KNAT1 and ERECTA regulate inflorescence architecture in Arabidopsis. Plant Cell **14:** 547–558.

Felsenstein, J. (1981). Evolutionary trees from DNA sequences - A maximum-likelihood approach. J. Mol. Evol. **17:** 368–376.

Fields, S., and Song, O.K. (1989). A novel genetic system to detect protein-protein interactions. Nature **340:** 245–246.

Gleave, A.P. (1992). A versatile binary vector system with a T-DNA organizational structure conducive to efficient integration of cloned DNA into the plant genome. Plant Mol. Biol. **20:** 1203–1207.

Guindon, S., and Gascuel, O. (2003). A simple, fast, and accurate algorithm to estimate large phylogenies by maximum likelihood. Syst. Biol. **52:** 696–704.

Guindon, S., Lethiec, F., Duroux, P., and Gascuel, O. (2005). PHYML online - A web server for fast maximum likelihood-based phylogenetic inference. Nucleic Acids Res. **33:** W557–W559.

Hackbusch, J., Richter, K., Muller, J., Salamini, F., and Uhrig, J.F. (2005). A central role of *Arabidopsis thaliana* ovate family proteins in networking and subcellular localization of 3-aa loop extension homeodomain proteins. Proc. Natl. Acad. Sci. USA **102:** 4908–4912.

Hall, T.A. (1999). BioEdit: A user-friendly biological sequence alignment editor and analysis program for Windows 95/98/NT. Nucleic Acids Symp. Ser. **41:** 95–98.

Hay, A., Jackson, D., Ori, N., and Hake, S. (2003). Analysis of the competence to respond to KNOTTED1 activity in Arabidopsis leaves using a steroid induction system. Plant Physiol. **131:** 1671–1680.

Hay, A., and Tsiantis, M. (2006). The genetic basis for differences in leaf form between *Arabidopsis thaliana* and its wild relative *Cardamine hirsuta*. Nat. Genet. **38:** 942–947.

Henikoff, S., and Henikoff, J.G. (1992). Amino-acid substitution matrices from protein blocks. Proc. Natl. Acad. Sci. USA **89:** 10915–10919.

Hepworth, S.R., Zhang, Y.L., Mckim, S., Li, X., and Haughn, G. (2005). BLADE-ON-PETIOLE-dependent signaling controls leaf and floral patterning in Arabidopsis. Plant Cell **17:** 1434–1448.

Iwakawa, H., Ueno, Y., Semiarti, E., Onouchi, H., Kojima, S., Tsukaya, H., Hasebe, M., Soma, T., Ikezaki, M., Machida, C., and Machida, Y. (2002). The ASYMMETRIC LEAVES2 gene of *Arabidopsis thaliana*, required for formation of a symmetric flat leaf lamina, encodes a member of a novel family of proteins characterized by cysteine repeats and a leucine zipper. Plant Cell Physiol. **43:** 467–478.

Jefferson, R.A., Kavanagh, T.A., and Bevan, M.W. (1987). GUS fusions: Beta-glucuronidase as a sensitive and versatile gene fusion marker in higher plants. EMBO J. **6:** 3901–3907.

Kanrar, S., Onguka, O., and Smith, H.M. (2006). Arabidopsis inflorescence architecture requires the activities of KNOX-BELL homeodomain heterodimers. Planta **224:** 1163–1173.

Kim, J.Y., Rim, Y., Wang, L., and Jackson, D. (2005). A novel cell-to-cell trafficking assay indicates that the KNOX homeodomain is necessary and sufficient for intercellular protein and mRNA trafficking. Genes Dev. **19:** 788–793.

Kim, J.Y., Yuan, Z., and Jackson, D. (2003). Developmental regulation and significance of KNOX protein trafficking in Arabidopsis. Development **130:** 4351–4362.

Kim, M., Canio, W., Kessler, S., and Sinha, N. (2001). Developmental changes due to long-distance movement of a homeobox fusion transcript in tomato. Science **293:** 287–289.

Kohalmi, S.E., Reader, L.J.W., Samach, A., Nowak, J., Haughn, G.W., and Crosby, W.L. (1988). Identification and characterization of protein interactions using the yeast 2-hybrid system. In Plant Molecular Biology Manual M1, S.B. Gelvin and R.A. Schilperoort, eds (Dordrecht, The Netherlands: Kluwer Academic Publishers), pp. 1–30.

Lincoln, C., Long, J., Yamaguchi, J., Serikawa, K., and Hake, S. (1994). A knotted1-like homeobox gene in Arabidopsis is expressed in the vegetative meristem and dramatically alters leaf morphology when overexpressed in transgenic plants. Plant Cell **6:** 1859–1876.

Long, J.A., Moan, E.I., Medford, J.I., and Barton, M.K. (1996). A member of the KNOTTED class of homeodomain proteins encoded by the STM gene of Arabidopsis. Nature **379:** 66–69.

Mattsson, J., Ckurshumova, W., and Berleth, T. (2003). Auxin signaling in Arabidopsis leaf vascular development. Plant Physiol. **131:** 1327–1339.

McCallum, C.M., Comai, L., Greene, E.A., and Henikoff, S. (2000). Targeting induced local lesions in genomes (TILLING) for plant functional genomics. Plant Physiol. **123:** 439–442.

Mclellan, T., and Dengler, N. (1995). Pattern and form in repeated elements in the development of simple leaves of *Begonia dregei*. Int. J. Plant Sci. **156:** 581–589.

Modrusan, Z., Reiser, L., Feldmann, K.A., Fischer, R.L., and Haughn, G.W. (1994). Homeotic transformation of ovules into carpel-like structures in Arabidopsis. Plant Cell **6:** 333–349.

Muller, J., Wang, Y., Franzen, R., Santi, L., Salamini, F., and Rohde, W. (2001). In vitro interactions between barley TALE homeodomain proteins suggest a role for protein-protein associations in the regulation of Knox gene function. Plant J. **27:** 13–23.

Narita, N.N., Moore, S., Horiguchi, G., Kubo, M., Demura, T., Fukuda, H., Goodrich, J., and Tsukaya, H. (2004). Overexpression of a novel small peptide ROTUNDIFOLIA4 decreases cell proliferation and alters leaf shape in *Arabidopsis thaliana*. Plant J. **38:** 699–713.

Nikovics, K., Blein, T., Peaucelle, A., Ishida, T., Morin, H., Aida, M., and Laufs, P. (2006). The balance between the MIR164A and CUC2 genes controls leaf margin serration in Arabidopsis. Plant Cell **18:** 2929–2945.

Ori, N., Eshed, Y., Chuck, G., Bowman, J.L., and Hake, S. (2000). Mechanisms that control knox gene expression in the Arabidopsis shoot. Development **127:** 5523–5532.

Pautot, V., Dockx, J., Hamant, O., Kronenberger, J., Grandjean, O., Jublot, D., and Traas, J. (2001). KNAT2: Evidence for a link between knotted-like genes and carpel development. Plant Cell **13:** 1719–1734.

Pelaz, S., Ditta, G.S., Baumann, E., Wisman, E., and Yanofsky, M.F. (2000). B and C floral organ identity functions require SEPALLATA MADS-box genes. Nature **405:** 200–203.

Quaedvlieg, N., Dockx, J., Rook, F., Weisbeek, P., and Smeekens, S. (1995). The homeobox gene ATH1 of Arabidopsis is derepressed in the photomorphogenic mutants cop1 and det1. Plant Cell **7:** 117–129.

Reiser, L., Modrusan, Z., Margossian, L., Samach, A., Ohad, N., Haughn, G.W., and Fischer, R.L. (1995). The BELL1 gene encodes a homeodomain protein involved in pattern formation in the Arabidopsis ovule primordium. Cell **83:** 735–742.

Robinson-Beers, K., Pruitt, R.E., and Gasser, C.S. (1992). Ovule development in wild-type Arabidopsis and two female-sterile mutants. Plant Cell **4:** 1237–1249.

Roeder, A.H., Ferrandiz, C., and Yanofsky, M.F. (2003). The role of the REPLUMLESS homeodomain protein in patterning the Arabidopsis fruit. Curr. Biol. **13:** 1630–1635.

Samach, A., Kohalmi, S.E., Motte, P., Datla, R., and Haughn, G.W. (1997). Divergence of function and regulation of class B floral organ identity genes. Plant Cell **9:** 559–570.

Semiarti, E., Ueno, Y., Tsukaya, H., Iwakawa, H., Machida, C., and Machida, Y. (2001). The ASYMMETRIC LEAVES2 gene of *Arabidopsis thaliana* regulates formation of a symmetric lamina, establishment

of venation and repression of meristem-related homeobox genes in leaves. Development **128:** 1771–1783.

Serrano-Cartagena, J., Robles, P., Ponce, M.R., and Micol, J.L. (1999). Genetic analysis of leaf form mutants from the Arabidopsis Information Service collection. Mol. Gen. Genet. **261:** 725–739.

Sieburth, L.E., and Meyerowitz, E.M. (1997). Molecular dissection of the AGAMOUS control region shows that cis elements for spatial regulation are located intragenically. Plant Cell **9:** 355–365.

Smith, H.M., Boschke, I., and Hake, S. (2002). Selective interaction of plant homeodomain proteins mediates high DNA-binding affinity. Proc. Natl. Acad. Sci. USA **99:** 9579–9584.

Smith, H.M., Campbell, B.C., and Hake, S. (2004). Competence to respond to floral inductive signals requires the homeobox genes PENNYWISE and POUND-FOOLISH. Curr. Biol. **14:** 812–817.

Smith, H.M., and Hake, S. (2003). The interaction of two homeobox genes, BREVIPEDICELLUS and PENNYWISE, regulates internode patterning in the Arabidopsis inflorescence. Plant Cell **15:** 1717–1727.

Smyth, D.R., Bowman, J.L., and Meyerowitz, E.M. (1990). Early flower development in Arabidopsis. Plant Cell **2:** 755–767.

Thompson, J.D., Gibson, T.J., Plewniak, F., Jeanmougin, F., and Higgins, D.G. (1997). The CLUSTAL_X windows interface: Flexible strategies for multiple sequence alignment aided by quality analysis tools. Nucleic Acids Res. **25:** 4876–4882.

Thompson, J.D., Higgins, D.G., and Gibson, T.J. (1994). CLUSTAL W: Improving the sensitivity of progressive multiple sequence alignment through sequence weighting, position-specific gap penalties and weight matrix choice. Nucleic Acids Res. **22:** 4673–4680.

Till, B.J., Burtner, C., Comai, L., and Henikoff, S. (2004). Mismatch cleavage by single-strand specific nucleases. Nucleic Acids Res. **32:** 2632–2641.

Tsukaya, H., and Uchimiya, H. (1997). Genetic analyses of the formation of the serrated margin of leaf blades in Arabidopsis: Combination of a mutational analysis of leaf morphogenesis with the characterization of a specific marker gene expressed in hydathodes and stipules. Mol. Gen. Genet. **256:** 231–238.

Venglat, S.P., Dumonceaux, T., Rozwadowski, K., Parnell, L., Babic, V., Keller, W., Martienssen, R., Selvaraj, G., and Datla, R. (2002). The homeobox gene BREVIPEDICELLUS is a key regulator of inflorescence architecture in Arabidopsis. Proc. Natl. Acad. Sci. USA **99:** 4730–4735.

Western, T.L., Young, D.S., Dean, G.H., Tan, W.L., Samuels, A.L., and Haughn, G.W. (2004). MUCILAGE-MODIFIED4 encodes a putative pectin biosynthetic enzyme developmentally regulated by APETALA2, TRANSPARENT TESTA GLABRA1, and GLABRA2 in the Arabidopsis seed coat. Plant Physiol. **134:** 296–306.

Xu, L., Xu, Y., Dong, A., Sun, Y., Pi, L., Xu, Y., and Huang, H. (2003). Novel as1 and as2 defects in leaf adaxial-abaxial polarity reveal the requirement for ASYMMETRIC LEAVES1 and 2 and ERECTA functions in specifying leaf adaxial identity. Development **130:** 4097–4107.